A Full Physics Real-Time Solver for Simulating Arrhythmias in the Human Heart

Thomas Schrotter[1], Matthias AF Gsell[1], Aurel Neic[2], Gernot Plank[1]

[1] Medical University of Graz, Austria
[2] NumeriCor GmbH, Graz, Austria

Abstract

For simulating human cardiac electrophysiology (CEP), the bidomain model is considered the gold standard owing to its ability to replicate experimental observations with high fidelity. However, its reaction-diffusion (RD) nature and associated constraints on spatiotemporal discretization result in significant computational costs, limiting its adoptions in industrial and clinical applications. Eikonal-based models are computationally more efficient but lack the capability to accurately simulate cardiac arrhythmias. We present a real-time capable reentrant eikonal model (REK) that combines an eikonal solver with a finite state machine (FSM) to track action potential phases and incorporates physiological restitution, curvature and diffusion effects, as measured in a high fidelity reference RD model. Local activation times (LATs), conduction velocities (CVs) and local repolarization times (LRTs) measured in infarct simulations were compared against baseline RD monodomain solutions, where low root mean square errors (RMSEs) of $2.4\,\mathrm{ms}$, $1.6\,\mathrm{mm/s}$ *and* $6.8\,\mathrm{ms}$ *were reported, respectively. Reconstructed transmembrane voltages and electro-cardiograms (ECGs) qualitatively agree closely with the baseline solution, while offering a speedup of* $\sim$420*. Our results demonstrate that the REK model is capable of simulating cardiac arrhythmias in real-time, matching monodomain solutions with minor deviations.*

1. Introduction

Computational models of CEP are increasingly being applied in a broad range of industrial and clinical contexts. The biophysically detailed RD bidomain model is widely regarded as the gold standard for modeling human CEP at both tissue and organ scales. However, RD models are vastly expensive to solve due to the spatiotemporal discretization constraints imposed by RD mechanisms for mediating wavefront propagation. Simpler pseudo-bidomain or monodomain models are computationally an order of magnitude cheaper [1], but remain hampered by these constraints, rendering RD-based models unfeasible for time-critical clinical applications. Reaction-eikonal (RE) models are able to lift these constraints by complementing the mediating wavefront propagation based on diffusion by a prescribed eikonal-based activation mechanism [2]. Such models can be discretized at spatial resolutions of $\approx 1\,\mathrm{mm}$ at which model execution with real-time performance is achievable. Nevertheless, RE models are unable to capture repetitive or reentrant activation sequences where physiological features such as CV, action potential duration (APD) and excitability exhibit history dependent behavior.

In this study, we introduce a novel real-time capable REK model that closely matches biophysically detailed RD monodomain simulations. The model leverages an eikonal solver coupled to a FSM that tracks and controls CEP properties in a history-dependent manner. Critically, CEP properties governing repetitive activation and repolarization, as well as initiation and maintenance of arrhythmias, are measured in a high fidelity monodomain RD model and mapped onto the REK model during calibration. Validity of the REK model is evaluated through quantitative and qualitative comparisons between monodomain and REK simulations under infarct scenarios relevant for modeling arrhythmias at the organ scale. Our results demonstrate that the REK model can accurately replicate repetitive and reentrant activation-repolarization sequences computed by the monodomain model while maintaining real-time performance and biophysical fidelity.

2. Methods

We seek to develop a multi-frontal REK model that is able to closely match a full physics RD-based CEP model at real-time performance, including reentrant activation and repolarization patterns of both anatomical and functional type. This requires the consideration of emergent physical features of physiological RD models, which include exciteability, the CV dependence on wavefront curvature and restitution, as well as the influence of APD restitution and electrotonic currents on repolarization.

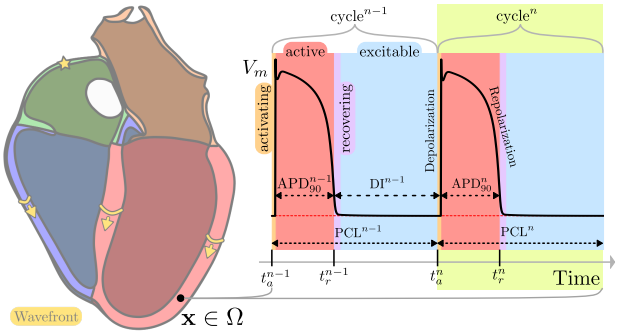

Figure 1. A time trace of the transmembrane voltage V_m at a point $\mathbf{x} \in \Omega$ is shown. The n-th depolarization wavefront arriving at $\mathbf{x}$ at time t_a^n marks the start of the n-th cycle.

2.1. Physiology Dependence of the CV

In a physiological RD model, CV depends on excitability, the recovery state after a preceding instant of repolarization, the curvature of the propagating depolarization wavefront and the electrotonic load imposed by tissue downstream along the direction of propagation, modulated by boundary conditions. Assuming that the n-th depolarization wavefront is arriving at location $\mathbf{x} \in \Omega$ (see Fig. 1), the CV at that point can be described by a symmetric velocity tensor $\mathbf{V}^n : \Omega \to \mathbb{R}^{3\times3}$ which is derived from the domain's orthonormal eigenaxes, $\zeta \to \mathbf{f}(\mathbf{x}), \mathbf{s}(\mathbf{x}), \mathbf{n}(\mathbf{x}) \in \mathbb{R}^3$, along the fiber, sheet, and sheet-normal direction, as

$$\mathbf{V}^n = v_f^{n2}\,(\mathbf{f}\otimes\mathbf{f}) + v_s^{n2}\,(\mathbf{s}\otimes\mathbf{s}) + v_n^{n2}\,(\mathbf{n}\otimes\mathbf{n})\,, \quad (1)$$

where the eigenvalues of the velocity tensor $\mathbf{V}$ along the eigenaxes ζ are given by

$$\begin{aligned} v_\zeta^n &= v_{0,\zeta}\cdot f_{\mathrm{CVR},\zeta}\left(\mathrm{PCL}^{n-1}\right)\cdot f_{\mathrm{CVK},\zeta}\left(\kappa^n\right), \\ \mathrm{PCL}^{n-1} &= t_a^n - t_a^{n-1}, \qquad \kappa^n = -\nabla\cdot\frac{\nabla t_a^n}{\|\nabla t_a^n\|}, \end{aligned} \quad (2)$$

and where the relative restitution curve $f_{\mathrm{CVR},\zeta}$ governs the dependence of CV on the pacing cycle length (PCL) of the preceding $(n-1)$-th cycle. $v_{0,\zeta}$ is the CV of a planar wavefront propagating along direction ζ at long diastolic intervals (DIs). $f_{\mathrm{CVK},\zeta}$ describes the dependence of CV on the wavefront curvature $\kappa \in \mathbb{R}$.

2.2. Physiology Dependence of the APD

The cardiac APD is governed by cellular restitution effects which depend on the DI between two consecutive cycles. This effect can be taken into account in the form of a tissue-level APD restitution curve, f_{APD}, given by

$$\begin{aligned} \mathrm{DI}^{n-1} &= \mathrm{PCL}^{n-1} - \mathrm{APD}_{90}^{n-1}, \\ \mathrm{APD}_{90}^{n} &= f_{\mathrm{APD}}\left(\mathrm{DI}^{n-1}\right). \end{aligned} \quad (3)$$

Furthermore, the repolarization at each point $\mathbf{x} \in \Omega$, described by a value $R^n \in [0,1]$, given by

$$R^n = \max\left(0, \min\left(\frac{t - t_a^n}{\mathrm{APD}_{100}^n}, 1\right)\right), \quad (4)$$

is precipitated or slowed down by adjacent tissue due to electrotonic loading. This effect is approximated by

$$\overline{\mathrm{R}}^n = \Delta_{\mathbf{\Lambda}}\left(R^n\right), \quad \overline{\mathrm{APD}}_{90}^n = \Delta_{\mathbf{\Lambda}}\left(\mathrm{APD}_{90}^n\right), \quad (5)$$

where $\Delta_{\mathbf{\Lambda}}$ acts as a smoothing operator within a given electrotonic distance governed by the space constant tensor $\mathbf{\Lambda} = \mathrm{diag}(\lambda_f, \lambda_s, \lambda_n)$ and the fiber alignment.

2.3. EP-informed Reentrant-Eikonal Model

An anisotropic eikonal model accounting for the dependence of CV of depolarization wavefronts, as in Eq. (1), travelling in a domain $\Omega \subset \mathbb{R}^3$ takes the form

$$\begin{aligned} \sqrt{\nabla t_\mathrm{a}\cdot\mathbf{V}\nabla t_\mathrm{a}} &= 1 \quad \text{in } \Omega \\ t_\mathrm{a} &= t_0 \quad \text{in } \Gamma \end{aligned} \quad (6)$$

with $\Gamma \subset \Omega$ and prescribed arrival times t_0 given in Γ. This model is coupled to a FSM that keeps track of the action potential phases relative to each instant of activation (see Fig. 2). During the depolarization phase, the REK model expands the wavefront by solving Eq. (6) for each time step Δt using the Fast Iterative Method [3]. Upon activation, the initial APD is determined by APD restitution, as in Eq. (3). During the repolarization phase, diffusion influences the nodal repolarization R^n according to Eq. (5) and the FSM updates all states and controls the excitability of each $\mathbf{x} \in \Omega$ for each cycle n, allowing multi-frontal activation times $t_\mathrm{a}(\mathbf{x}) := \{t_a^n(\mathbf{x}) \mid n \in \mathbb{N}, t_a^{n-1}(\mathbf{x}) < t_a^n(\mathbf{x})\}$ and therefore reentrant wave propagation.

2.4. Translation of Cardiac Sources

Cardiac sources in the form of transmembrane voltages, $V_\mathrm{m}(\mathbf{x}, t)$, are translated using a prescribed action potential $f_{\mathrm{AP}} : (\mathbb{R}, \mathbb{R}) \to \mathbb{R}$. The transmembrane voltage at a point $\mathbf{x} \in \Omega$ at a given instant in time t within the n-th cycle can then be recovered by

$$V_\mathrm{m}^n(\mathbf{x}, t) = f_{\mathrm{AP}}\left(\overline{\mathrm{R}}^n(\mathbf{x}), \overline{\mathrm{APD}}_{90}^n(\mathbf{x})\right). \quad (7)$$

2.5. Model Calibration

The CEP properties considered within the REK model were quantitatively measured on a high fidelity 250 µm RD monodomain model using the ForCEPSS framework [4]. The REK model was calibrated for the two cardiac tissue

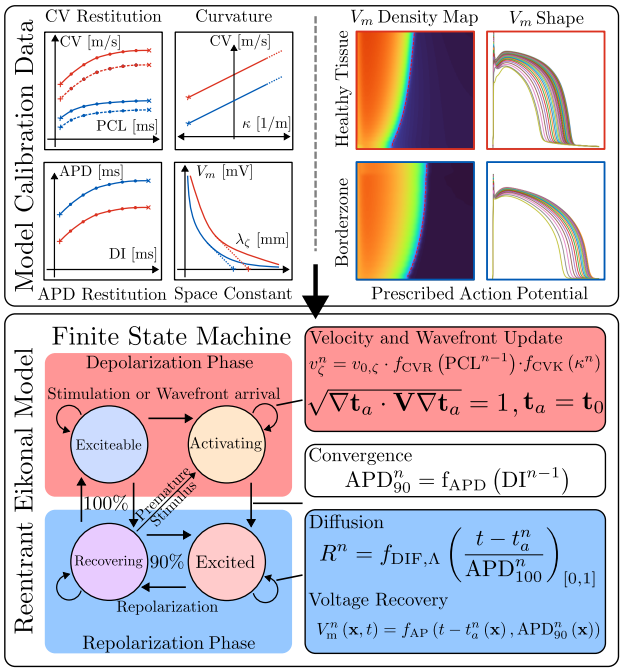

Figure 2. REK model overview. FSM states and transitions are derived from the cardiac action potential in Fig. 1.

types described in the ForCEPSS paper, healthy and borderzone. The prescribed action potential shapes f_{AP} and restitution functions f_{APD} were obtained from myocyte simulations, whereas the dependence of CV to restitution $f_{\mathrm{CVR},\zeta}$ and curvature $f_{\mathrm{CVK},\zeta}$, as well as the space constant tensor $\mathbf{\Lambda}$, was derived from tissue simulations (see Fig. 2).

3. Model Validation

The ability of the calibrated REK model to replicate CEP behaviours observed in RD-based models was evaluated by comparing REK simulations to ground-truth monodomain simulations generated using openCARP [5], in two scenarios, depicted in Figure 3.

(A) Over a 5 second simulation window, an infarct-mediated reentry was induced in a high fidelity 250 µm, thin 3D sheet of healthy ventricular tissue containing an isthmus-shaped scar with a 2 mm borderzone by applying an S1-S2 protocol, as described in [4]. Differences between the monodomain and the REK simulation were quantified by computing and visualizing the error between nodal LAT, CV, LRT and APD maps. LATs and LRTs in monodomain simulations were determined as the instants in time when the transmembrane voltage of a depolarization wavefront or a repolarization waveback crossed a threshold of $V_{\mathrm{th}} = -75mV$ with a positive or negative slope, respectively. CV maps were derived by inverting the norm of the delay vector computed as the gradient of the

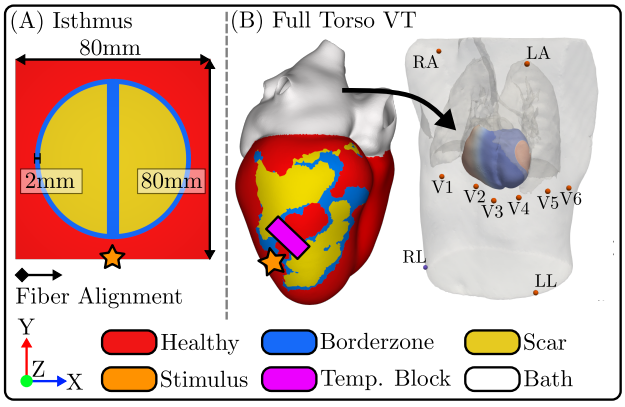

Figure 3. Evaluation geometries and stimulation sites. Stimuli were applied using a 2 ms voltage clamp to 0 mV.

activation map, that is $v^n(\mathbf{x}) = ||\nabla t_{\mathrm{a}}^n(\mathbf{x})||_2^{-1}$. Recovered transmembrane voltages were qualitatively compared between both methods to highlight differences in reentrant activation and repolarization patterns.

(B) A ventricular tachycardia (VT) was induced in an anatomically accurate full-torso cardiac model [6] containing an isthmus-shaped scar by forcing unidirectional propagation using a temporal block located at one isthmus entrance. Spatial fidelity was 250 µm for the monodomain simulation and 1200 µm for the REK simulation. Over a 5 second simulation window, 12-lead ECGs from both models were recovered from transmembrane voltages using lead field reconstruction [7] and qualitatively compared. Finally, the required computation times were measured.

4. Results

(A) The error density histograms in Figure 4 indicate that the REK model closely approximates the monodomain model, with reported LAT, CV, LRT and APD RMSEs of 2.4 ms, 1.6 mm/s, 6.8 ms and 6.9 ms, respectively. Observed activation, repolarization and reentry patterns in Figure 5 matched qualitatively well between the monodomain and the REK model.

(B) High similarity between the recovered ECGs of the monodomain and the REK model was observed in Figure 6, with minor differences in signal morphology and amplitude evident in leads II, V4-V6 and maVR. The reported computation times were ~14 hours for the monodomain and ~2 minutes for the REK simulation, resulting in a speedup of ~420.

5. Conclusion

Our evaluation of the REK model demonstrates its ability to accurately match activation, repolarization, and reentry patterns observed in high fidelity monodomain simu-

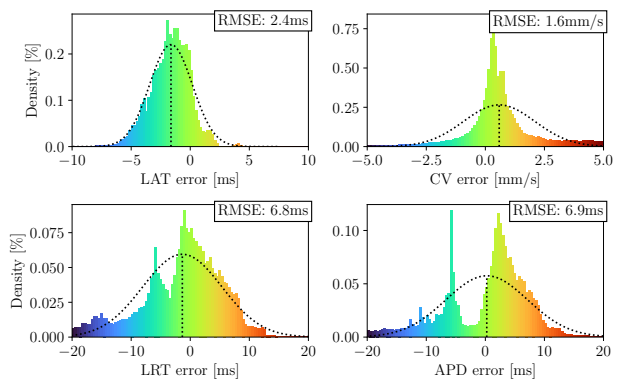

Figure 4. Error density histograms and corresponding RMSEs of LATs, CVs, LRTs and APDs measured between the monodomain and the REK model in the isthmus scenario **(A)**. A bin size of 100 was used for the histograms.

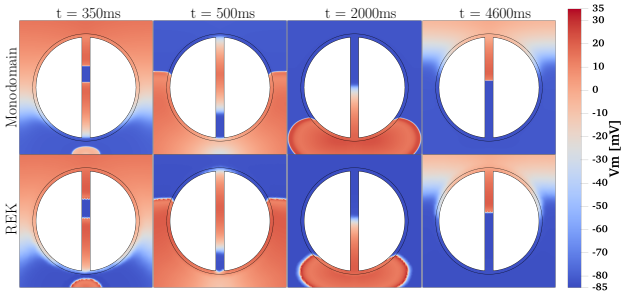

Figure 5. Activation, repolarization and reentry pattern comparison between transmembrane voltage maps generated by the monodomain and the REK model in the isthmus scenario **(A)**. Both models sustained the reentry throughout the entire 5 second long simulation.

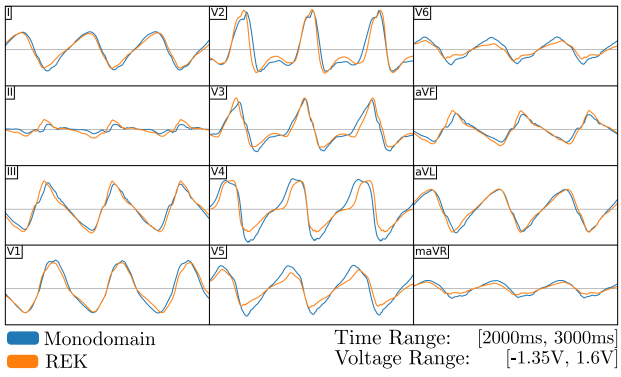

Figure 6. Recovered 12-lead ECG comparison between monodomain and the REK model during an induced VT in simulation **(B)**. The zoomed ECG window between 2-3 seconds highlights signal amplitude and morphology differences between both methods. In both cases, the VT was sustained throughout the entire 5 second long simulation.

lations with real-time performance. Reconstructed ECGs between both models were nearly identical. For the scenarios considered, differences were minor and well below the variability due to parameter uncertainty inherent in the monodomain model. Performance and fidelity of the REK model indicate its applicability in time-critical clinical applications, such as e.g. identifying VT circuits.

Acknowledgments

This research was funded by the InstaTwin grant FO999891133 from the Austrian Research Promotion Agency (FFG).

References

[1] Bishop MJ, Plank G. Bidomain ECG simulations using an augmented monodomain model for the cardiac source. IEEE Transactions on Biomedical Engineering 2011;58(8):2297–2307.

[2] Neic A, Campos FO, Prassl AJ, Niederer SA, Bishop MJ, Vigmond EJ, Plank G. Efficient computation of electrograms and ECGs in human whole heart simulations using a reaction-eikonal model. Journal of Computational Physics 2017;346:191–211.

[3] Fu Z, Kirby RM, Whitaker RT. A fast iterative method for solving the eikonal equation on tetrahedral domains. SIAM Journal on Scientific Computing 2013;35(5):C473–C494.

[4] Gsell MA, Neic A, Bishop MJ, Gillette K, Prassl AJ, Augustin CM, Vigmond EJ, Plank G. ForCEPSS - A framework for cardiac electrophysiology simulations standardization. Computer Methods and Programs in Biomedicine 2024; 251:108189.

[5] Plank G, Loewe A, Neic A, Augustin C, Huang YL, Gsell MA, Karabelas E, Nothstein M, Prassl AJ, Sánchez J, et al. The openCARP simulation environment for cardiac electrophysiology. Computer Methods and Programs in Biomedicine 2021;208:106223.

[6] Gillette K, Gsell MA, Prassl AJ, Karabelas E, Reiter U, Reiter G, Grandits T, Payer C, Štern D, Urschler M, et al. A framework for the generation of digital twins of cardiac electrophysiology from clinical 12-leads ECGs. Medical Image Analysis 2021;71:102080.

[7] Potse M. Scalable and accurate ECG simulation for reaction-diffusion models of the human heart. Frontiers in Physiology 2018;9:370.

Address for correspondence:

Dipl.-Ing. Thomas Schrotter
Gottfried Schatz Research Center
Division of Medical Physics and Biophysics
Neue Stiftingtalstraße 6/IV
8010 Graz, Austria
thomas.schrotter@medunigraz.at